Development 134, 557-565 (2007) doi:10.1242/dev.02741

The mouse seminal vesicle shape mutation is allelic with *Fgfr2*

Sheri L. Kuslak, Joshua L. Thielen and Paul C. Marker*

The mouse seminal vesicle shape (svs) mutation is a spontaneous recessive mutation that causes branching morphogenesis defects in the prostate gland and seminal vesicles. Unlike many other mutations that reduce prostatic and/or seminal vesicle branching, the svs mutation dramatically reduces branching without reducing organ growth. Using a positional cloning approach, we identified the svs mutant lesion as a 491 bp insertion in the tenth intron of *Fgfr2* that results in changes in the pattern of *Fgfr2* alternative splicing. An engineered null allele of *Fgfr2* failed to complement the svs mutation proving that a partial loss of FGFR2(IIIb) isoforms causes svs phenotypes. Thus, the svs mutation represents a new type of adult viable *Fgfr2* allele that can be used to elucidate receptor function during normal development and in the adult. In the developing seminal vesicles, sustained activation of ERK1/2 was associated with branching morphogenesis and this was absent in svs mutant seminal vesicles. This defect appears to be the immediate downstream effect of partial loss of FGFR2(IIIb) because activation of FGFR2(IIIb) by FGF10 rapidly induced ERK1/2 activation, and inhibition of ERK1/2 activation blocked seminal vesicle branching morphogenesis. Partial loss of FGFR2(IIIb) was also associated with down-regulation of several branching morphogenesis regulators including *Shh*, *Ptch1*, *Gli1*, *Gli2*, *Bmp4*, and *Bmp7*. Together with previous studies, these data suggest that peak levels of FGFR2(IIIb) signaling are required to induce branching and sustain ERK1/2 activation, whereas reduced levels support ductal outgrowth in the prostate gland and seminal vesicles.

KEY WORDS: *Fgfr2*, Prostate, Seminal vesicle, Branching morphogenesis, *Shh*, *Gli1*, *Fgf10*, *Gli2*, *Ptch1*, *Bmp4*, *Bmp7*, svs, Seminal vesicle shape mutation

INTRODUCTION

The mouse seminal vesicle shape (svs) mutation is a spontaneous recessive mutation that arose during the creation of the mouse CXB5 recombinant inbred strain from parental strains Balb/cBy and C57BL/6By. The svs mutation is absent from the other CXB recombinant inbred lines and was first identified because it alters the adult morphology of the seminal vesicles (Shukri et al., 1988). The altered seminal vesicle morphology results from a complete failure of branching morphogenesis during seminal vesicle development (Marker et al., 2003a). In addition, the svs mutation reduces branching morphogenesis in the prostate gland by approximately 40% (Marker et al., 2003a), owing to increased ductal length between the bifurcation events of the elongating buds, resulting in a reduced number of ductal tips with no reduction in organ weight (Marker et al., 2003a).

Branching morphogenesis is a developmental process common to almost all organisms in the animal kingdom (Davies, 2002). In mammals, the kidney, lung and most glands including the pancreas, mammary, prostate and seminal vesicles undergo branching morphogenesis during development. Organogenesis of branched organs has been described in terms of five steps: organ specification, epithelial bud initiation, epithelial duct elongation into the mesenchyme, bifurcation of the ducts leading to complex branching patterns, and cellular differentiation of the newly branched structure (Affolter et al., 2003). During prostate and seminal vesicle development, the svs mutation specifically affects budding/branching morphogenesis because organ specification, ductal elongation and cellular differentiation are normal in both organs (Marker et al., 2003a; Shukri et al., 1988). This contrasts with many other spontaneous and engineered mutations that decrease both organ growth and branching simultaneously in the prostate and/or seminal vesicles. Examples include mutations affecting *Ar*, *Gdf7*, *Ghr*, *Fgf10*, *Hoxa13*, *Hoxd13*, *Igf1* and *Srd5a2* (Donjacour et al., 2003; Marker et al., 2003b; Settle et al., 2001). In cases where both growth and branching are affected, it is difficult to determine if branching morphogenesis defects reflect a direct requirement for the gene in regulating branching or indirect effects of compromised organ growth. Because the svs mutation affects branching and not growth, it provides a unique opportunity to investigate the molecular mechanisms that control branching morphogenesis in the prostate and seminal vesicles.

Previous work mapped the svs mutation to a 2.7 cM interval on mouse chromosome 7 that included the *Fgfr2* locus (Marker et al., 2003a). *Fgfr2* was initially considered as a candidate for the gene affected by the svs mutation, and the *Fgfr2* open reading frame was sequenced but no changes were identified. This was not surprising because there was an apparent disconnect between phenotypes of known *Fgfr2* mutations and the phenotypes present in svs mutant mice. All previously reported loss-of-function *Fgfr2* mutations in mice caused dysgenesis or agenesis of organs throughout the body that resulted in embryonic or perinatal lethality (Arman et al., 1998; Arman et al., 1999; De Moerlooze et al., 2000; Hajihosseini et al., 2001; Xu et al., 1998), whereas we had identified only branching defects in the urogenital tract of svs mice. Additionally, gain-of-function mutations in *FGFR2* cause several human diseases including Crouzon, Jackson-Weiss, Apert and Pfeiffer syndromes (Hajihosseini et al., 2001; Hertz et al., 2001; Robertson et al., 1998), whereas svs mutant mice do not display any of the phenotypes associated with these diseases. Furthermore, FGF7 and FGF10 were known to be expressed in the mesenchyme of the developing prostate and seminal vesicles and to act via FGFR2(IIIb) expressed

Department of Genetics, Cell Biology and Development, University of Minnesota Comprehensive Cancer Center, University of Minnesota, Minneapolis, MN 55455, USA.

*Author for correspondence (e-mail: marke032@umn.edu)

Accepted 14 November 2006

in the developing epithelium, and recombinant FGF7 or FGF10 stimulated both growth and branching of developing prostates and seminal vesicles in vitro acting at least in part as pro-proliferative signals for the epithelium (Alarid et al., 1994; Sugimura et al., 1996; Thomson and Cunha, 1999). These data suggested that FGFR2 signaling was crucial for prostate and seminal vesicle growth and therefore did not fit well with the lack of growth defects in svs mutant prostates and seminal vesicles. The requirement for FGF10/FGFR2(IIIb) signaling for prostate growth was subsequently confirmed by analysis of FGF10-knockout mice (Donjacour et al., 2003).

In order to understand the molecular basis for the branching morphogenesis defects present in svs mutant mice, we took a positional cloning approach to identify the affected gene. The map position of the svs mutation was narrowed to a 410 kb interval predicted to contain eight genes. All eight genes were investigated but no coding region sequence changes were identified. Investigation of non-coding sequences identified a 491 bp insertion in the tenth intron of *Fgfr2* as a candidate svs mutation. This insertion was associated with changes in the pattern of *Fgfr2* alternative splicing, and an engineered null allele of *Fgfr2* failed to complement the svs mutation proving that a partial loss of FGFR2(IIIb) isoforms causes svs phenotypes. In addition, signaling by FGFR2(IIIb) through ERK1/2 (MAPK3/1 – Mouse Genome Informatics) and expression of several genes that regulate branching were found to be defective in svs mutant mice.

MATERIALS AND METHODS

PCR

Taq polymerase (New England BioLabs) was used according to the manufacturer's instructions to type markers D7Mit66, D7Mit285, D7Mit164, D7Mit205, D7Mit103, D7Mit165, D7Mit134, D7Mit135, D7Mit43, D7Mit107 and D7Mit108 (Research Genetics) on progeny from a previously described intraspecific mouse cross (Marker et al., 2003a).

PCR primers to amplify the svs insertion were: outer-svs, 5′-GTGAAGACTGGAGCTGCCCAGT-3′ and 5′-AGTTCAATTCCTACCACCTATGCTG-3′; nested-svs, 5′-AAGCTCACGGCTCCTTTGG-3′ and 5′-GGCACCTGCACACATGTACTTATAA-3′.

Full-length *Fgfr2* cDNA was amplified by a dT-primed reverse transcription (RT) followed by a primary and then a nested PCR using High Fidelity Taq according to the manufacturer's guidelines (Invitrogen). Primary primers, 5′-AGCAGGAACAGCAGTAACAACAGC-3′ and 5′-ACACACGTGACAATATGCTTCCCAC-3′; nested primers, 5′-CCGCTCGAGCGGATTGGCACTGTGACCATGGTCAGCT-3′ and 5′-AAGGAAAAAAGCGGCCGCAAAAGGAAAACACTCATGTTTTAACACTGCCG-3′.

Southern blotting

Genomic DNA from svs mutant mice (Jackson Laboratories) and the two parental control strains Balb/cBy and C57BL/6By (Jackson Laboratories) was digested with *Bam*HI, separated on a 0.8% agarose gel, transferred to Hybond-N+ membrane and then probed with a fragment of *Fgfr2* comprising bases 1,024 to 2,254 of GenBank NM_201601.

Complementation test

svs mutant mice were crossed to β-Actin.CRE transgenic mice (Jackson Laboratories) as previously described (Lewandoski et al., 1997) to generate svs/svs; β-Actin.CRE mice. This group was crossed with $Fgfr2^{flox/flox}$ (a generous gift from D. Ornitz, Washington University, St Louis, MO) to generate cohorts of mice that were $Fgfr2^{flox}$/svs or $Fgfr2^{\Delta}$/svs;β-Actin.CRE. Animals were typed by PCR from genomic DNA.

Western blotting

Protein lysates were prepared by sonicating seminal vesicles or ventral prostates at 30% amplitude for 10 seconds (Ultrasonic Processor) in modified Ripa's buffer (50 mM Tris-HCl, 1% NP40, 0.25% sodium dodecyl sulfate (NaDOC), 150 mM NaCl, 1 mM EDTA) with protease inhibitor cocktail (Roche). 5 μg of protein was run on a 4-12% stacking polyacrylamide gel (BioRad) under denaturing conditions. Protein was transferred to PVDF membrane (Millipore), blocked with 1% BSA in TBS, then probed with anti-FGFR2 (SantaCruz, sc-122), anti-FGFR2 (Sigma, F6796), anti-actin (Santa Cruz, sc-1616), anti-P-ERK1/2 (Cell Signaling Technologies, #9101), or anti-ERK1/2 (Cell Signaling Technologies, #9102) antibodies. Proteins were visualized by enhanced chemiluminesence exposed to film. Signal on film was quantified using a BioRad Gel Doc GS700 imaging densitometer.

In-situ hybridization

An *Fgfr2* partial cDNA (39,464-39,833 of GenBank AC157606) was used to synthesize DIG-labeled sense and antisense RNA probes using a DIG RNA Labeling Kit (Roche) according to the manufacturer's instructions. Fresh tissues were dissected in PBS at 4°C and embedded into OCT. Tissue sections (12 μm) were cut, mounted on Superfrost-plus microscope slides (Fisher), hybridized with the *Fgfr2* probe, and visualized as previously described (Thut et al., 2001).

Organ cultures

Postnatal day (P) 1 or 5 seminal vesicles were dissected out of CD1 mice (Charles River Laboratories) into basal medium at 4°C, and cultured in 5% CO_2 at 37°C on Millicell-CM Culture Plate Inserts (30 mm, 0.4 μm pore size; Millipore Corp.) in Nunclon Multidish 4-well plates (Nunc A/C) at the air/medium interface. Plate inserts were floated upon 0.5 ml of basal medium consisting of DMEM/F12 50/50 Mix supplemented with 0.37 g/L L-glutamine, 10 U/ml penicillin, 10 μg/ml streptomycin, 1×ITS, and 0.5% DMSO. Additional supplements included 2.5 μg/ml recombinant FGF10 (Peprotech Inc.), 1×10^{-8} M testosterone, and 20 μM UO126 (Cell Signaling Technologies). Culture medium was changed every other day during the culture period. To monitor branching, pictures were taken of organs on each day of culture.

Fgfr2 isoform analysis

Full-length *Fgfr2* amplicons and pIRES plasmid (Clontech) were digested with *Xho*I and *Not*I (New England BioLabs). pIRES was treated with shrimp alkaline phosphatase (Promega) and purified. *Fgfr2* amplicons were ligated into linear pIRES and transformed into *Escherichia coli* DH5α. Individual clones were characterized by restriction enzyme digestion and sequencing.

RNA isolation, RT-PCR and real-time PCR

Seminal vesicles were dissected from P5 svs mutant as well as heterozygous and wild-type littermate mice. Heterozygous and wild-type seminal vesicles were pooled and are referred to as wild type; svs mutant seminal vesicles were pooled and are referred to as mutant. Following dissection, pooled seminal vesicles were crushed in Trizol (Invitrogen) using a pestle and RNA isolated according to the manufacturer's instructions. Total RNA was amplified using the SMART RNA Amplification Kit (Clontech Laboratories) following the manufacturer's instructions.

For RT-PCR, 25 ng of poly(A) RNA was first treated with DNase according to the manufacturer's instructions (Invitrogen). Random primers, MMLV RT (Invitrogen) and other standard reagents were used in the PCR.

Real-time PCR was undertaken using a Lightcycler (Roche). Briefly, the LightCycler FastStart DNA MasterPLUS SYBR Green I Kit (Roche) was used with 5 μl of cDNA from the RT reaction. Primer sequences were as follows:

Shh, 5′-AATGCCTTGGCCATCTCTGT-3′ and 5′-GCTCGACCCTCATAGTGTAGAGACT-3′;

Ptch1, 5′-CTCTGGAGCAGATTTCCAAGG-3′ and 5′-TGCCGCAGTTCTTTTGAATG-3′;

Gli1, 5′-GGAAGTCCTATTCACGCCTTGA-3′ and 5′-CAACCTTCTTGCTCACACATGTAAG-3′;

Gli2, 5′-CCTTCTCCAATGCCTCAGAC-3′ and 5′-GGGGTCTGTGTACCTCTTGG-3′;

Bmp4, 5′-GGTTACCTCAAGGGAGTCGAGATTG-3′ and 5′-TCTTATTCTTCTTCCTGGACCGCTG-3′;

Bmp7, 5′-AGTGTGCCTTCCCTCTGAAC-3′ and 5′-AGGGCTTGGGTACGGTGT-3′.

Transcript levels were normalized to 18S RNA which was amplified using primer sequences 5′-GCCGCTAGAGGTGAAATTCTTG-3′ and 5′-CATTCTTGGCAAATGCTTTCG-3′. An analysis of variance (ANOVA) test was undertaken using StatView 4.1 (Abacus Concepts) to determine statistically significant differences.

Histology

Seminal vesicles from 9-month-old $Fgfr2^{flox}$/svs mice and $Fgfr2^{\Delta}$/svs mice were dissected into cold PBS and embedded in OCT. Tissue sections (12 μm) were cut using a cryostat, mounted on Superfrost-plus microscope slides, fixed in 100% ethanol at –20°C for 2 minutes, and allowed to dry at room temperature. Slides were stained with Hematoxylin and Eosin, dehydrated, and mounted using Permount.

RESULTS

Identification of a candidate svs mutation in the non-recombinant interval

We previously conducted an intraspecific backcross to map the location of the svs mutation on mouse chromosome 7 and localized the mutation to a 2.7 cM interval between *Tial1* and *Plekha1* (Marker et al., 2003a). We have now typed nine additional markers on the cross and localized the svs mutation to a 410 kb interval between D7Mit134 and D7Mit43 (Fig. 1A). Annotation of the mouse genome has identified two known and six predicted genes within this interval (Fig. 1B) (Birney et al., 2006; Waterston et al., 2002). We evaluated the candidate genes present between D7Mit134 and D7Mit43 for expression in the developing prostate and seminal vesicles by RT-PCR (data not shown). The predicted open reading frames for all detected candidate transcripts were sequenced in svs mutant mice and parental control strains Balb/cBy and C57BL/6By, but no changes were identified (data not shown). We subsequently initiated an effort to identify structural changes in the non-coding sequences of the candidate interval using Southern blotting. This identified a restriction fragment length polymorphism between svs mutant mice and the parental control strains Balb/cBy and C57BL/6By (Fig. 2A). The location of the polymorphism was predicted based on the mouse genome sequence, and subsequently analyzed by PCR (Waterston et al., 2002). The amplification of a longer fragment from svs mutant mice than from the two parental strains Balb/cBy and C57BL/6By suggested the presence of a novel insertion (Fig. 2B). Sequence analysis identified a 491 bp insertion identical to a murine leukemia virus long terminal repeat in the tenth intron of *Fgfr2* in svs mutant mice (Fig. 2C). This insertion was absent from all other CXB recombinant inbred strains of mice (data not shown), consistent with the possibility that this insertion is responsible for the phenotypes of svs mutant mice.

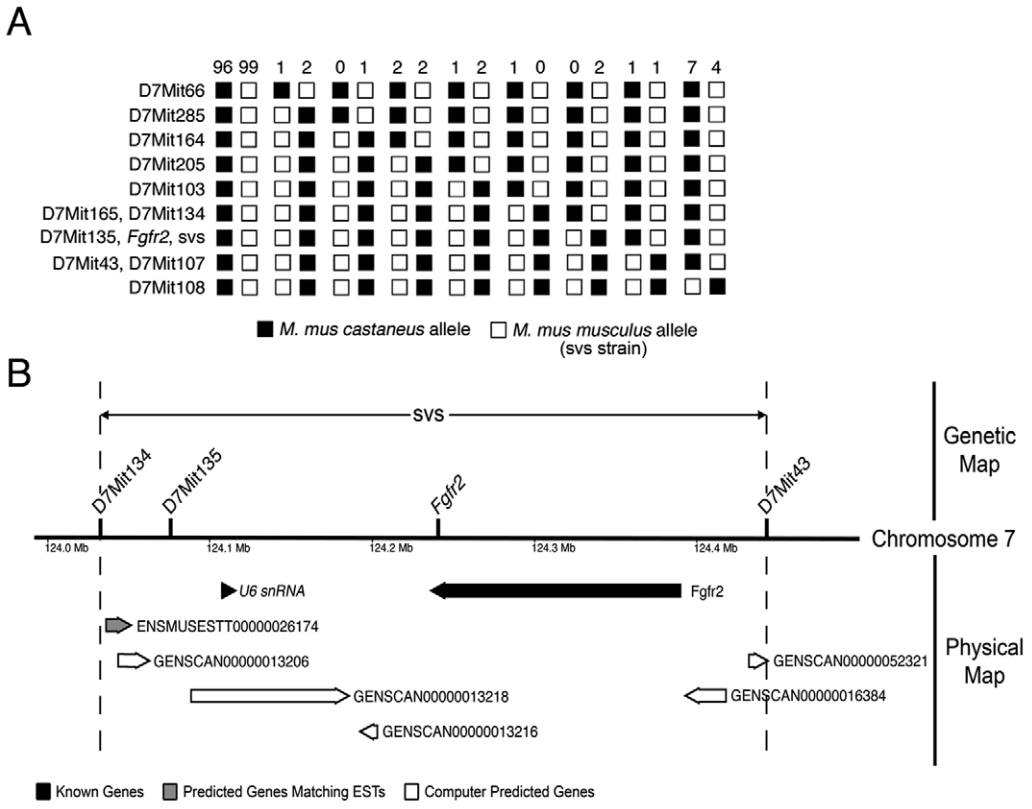

Fig. 1. Identification of a candidate svs mutation in a non-recombinant interval. (**A**) Block diagram showing the number of each chromosome type isolated in crosses between svs *M. mus musculus* and wild-type *M. mus castaneus* mice. Meiotic chromosomes typed for phenotypic and molecular loci are depicted as columns of blocks. White and black blocks indicate the presence of the *M. mus musculus* allele (svs strain) or the *M. mus castaneus* allele, respectively. The number of chromosomes observed with each genotype is shown at the top of the column (from a total of 222 informative chromosomes analyzed). Mapped loci are indicated on the left. (**B**) Genetic and physical maps of the svs candidate interval. The svs mutation maps between D7Mit134 and D7Mit43 on mouse chromosome 7 (top). In the NCBI m34 mouse genome sequence assembly (Waterston et al., 2002), this genetic interval corresponds to a 410.3 kb physical interval. Annotation of the genome sequence reveals the presence of two known and six predicted genes in this candidate interval (bottom) (Birney et al., 2006).

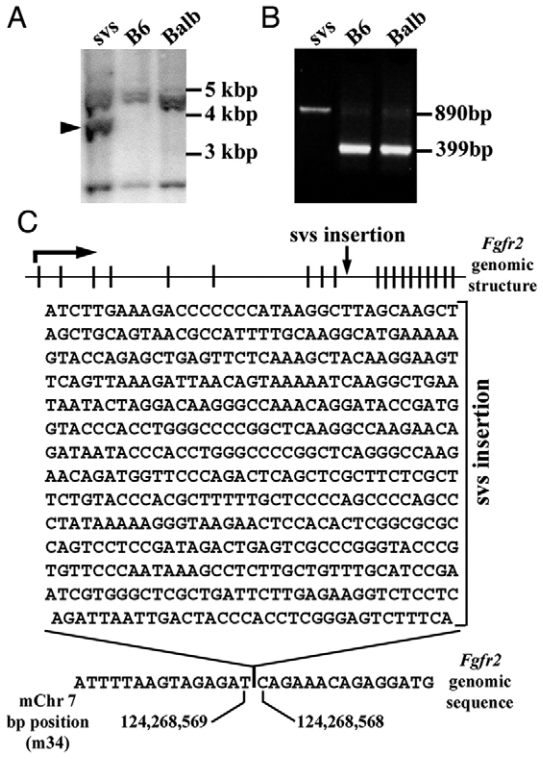

Fig. 2. Identification of a candidate svs mutation.
(**A**) Representative Southern blot of genomic DNA from svs, C57BL/6By (B6), and Balb/cBy (Balb) mice digested with *Bam*HI and probed with a fragment from *Fgfr2*. Note the shift of a major band only in svs mutant mice (arrowhead). (**B**) PCR of svs, C57BL/6By (B6), and Balb/cBy (Balb) mouse genomic DNA using primers flanking the candidate mutation. The parental control strains Balb/cBy and C57BL/6By have a 399 bp band, whereas svs mutant mice have an 890 bp band. (**C**) Genomic structure of *Fgfr2*. The horizontal arrow indicates the direction of transcription; the vertical lines indicate exons; and the vertical arrow indicates the intron which harbors the svs insertion (top). Sequencing of PCR products from svs mutant mice revealed a 491 bp insertion flanked by intronic *Fgfr2* sequences (bottom). Abbreviations: mChr7, mouse chromosome 7.

Partial loss of *Fgfr2* causes svs phenotypes

The potential consequences of this insertion for *Fgfr2* function were evaluated in several ways. Initially, we conducted western blot analysis using a commercially available antibody directed against the carboxy-terminus of FGFR2 and observed a banding pattern in both wild-type and svs mutant seminal vesicles similar to that previously reported for this antibody in experiments on other mouse tissues (Fig. 3A, upper panel). Previous reports indicate that these bands are specific for FGFR2 because they are eliminated in tissues with an engineered null mutation in FGFR2 (Xu et al., 1998), and they appear with the ectopic expression of FGFR2 cDNAs (Schmahl et al., 2004). In addition, a qualitatively similar result was obtained with a second antibody directed against the extracellular domain of FGFR2 (Yan et al., 2005) that strongly recognizes the lower molecular weight form of FGFR2 also recognized by the antibody directed against the carboxy terminus (Fig. 3A, middle panel). These data suggest that wild-type and svs mutant seminal vesicles express similar levels of FGFR2 protein. Furthermore, in situ hybridization using a probe directed against the first coding exon of *Fgfr2* showed that transcripts were correctly localized to the epithelium of the prostate and seminal vesicles in the control and svs mutant mice (Fig. 3B-D and data not shown).

Fgfr2 function is regulated by a complex pattern of alternative transcript splicing (Ingersoll et al., 2001). To determine if aberrant alternative splicing of *Fgfr2* was occurring in the svs mutant mice, full-length *Fgfr2* transcripts were amplified by RT-PCR from svs mutant and control P5 seminal vesicle RNA. A total of 111 control and 96 svs mutant full-length *Fgfr2* transcripts were analyzed by restriction enzyme digestion and sequencing. There was a surprisingly complex pattern of alternative splicing present in both control and svs mutant seminal vesicles. Eleven different isoforms were detected in each group, with only three isoforms overlapping between the control and svs mutant groups (Fig. 4A,B). The difference in isoform distribution between svs and control mice was highly statistically significantly (Pearson χ^2 test, $P<0.0001$). Strikingly, all of the *Fgfr2* transcripts expressed in control seminal vesicles included exon 8IIIb, which confers specificity for the FGF ligands expressed in the mesenchyme of the developing prostate and seminal vesicles (Thomson and Cunha, 1999). By contrast, 10 of 11 *Fgfr2* transcripts containing exon 8IIIb observed in wild-type seminal vesicles were reduced in or absent from svs mutant seminal vesicles.

To determine if partial loss of specific *Fgfr2* isoforms caused svs mutant phenotypes, a genetic complementation test was conducted using a previously described mutant allele of *Fgfr2*. This allele has exons 7, 8IIIb, 8IIIc and 9 (7-9) flanked by loxP sites ($Fgfr2^{flox}$) and encodes normal *Fgfr2* transcripts (Yu et al., 2003). However, in the presence of Cre recombinase, exons 7-9 are deleted and a null allele of *Fgfr2* is created ($Fgfr2^{\Delta}$). Crosses were conducted to create $Fgfr2^{flox}/svs$ and $Fgfr2^{\Delta}/svs$ mice. Seminal vesicles from both genotypes were evaluated for branching morphology at P5 (Fig. 5A-C) and by histology in adults (Fig. 5D,E). The $Fgfr2^{flox}$ allele complemented the svs mutation, but the $Fgfr2^{\Delta}$ allele did not, proving that svs phenotypes are due to a partial loss of *Fgfr2* function.

Signaling and gene expression change downstream of the svs mutation

FGFR2 is a receptor tyrosine kinase that can signal through multiple intracellular pathways (Chen et al., 2000; Kim et al., 2003; Nakamura et al., 2001; Newberry et al., 1997; Sakaguchi et al., 1999; Xiao et al., 2004; Yan et al., 1993). In the *Drosophila* trachea, the FGFR homolog *breathless* controls branching morphogenesis through the MEK-ERK pathway (Gabay et al., 1997; Lee et al., 1996; Sutherland et al., 1996). To investigate whether this pathway might be important for the phenotypes of svs mutant mice, the status of ERK1/2 activation was examined in svs mutant and control seminal vesicles. There was an abundance of phosphorylated ERK1/2 in control seminal vesicles whereas phosphorylated ERK1/2 could not be detected in svs mutant seminal vesicles (Fig. 6A). To determine if FGFR2(IIIb) directly activates ERK1/2 in developing seminal vesicles, wild-type organs were cultured with recombinant FGF10 protein. FGF10 is expressed by the developing mesenchyme of the prostate and seminal vesicles and can signal through the IIIb isoform of FGFR2 (Lu et al., 1999). FGF10 activated ERK1/2 in the wild-type seminal vesicles within 20 minutes, suggesting that this is a direct response of FGFR2(IIIb) activation (Fig. 6B). To determine if activated ERK1/2 is a plausible explanation for the loss of branching morphogenesis in the developing seminal vesicles of svs mutants, organ cultures of wild-type seminal vesicles were also conducted in the presence of

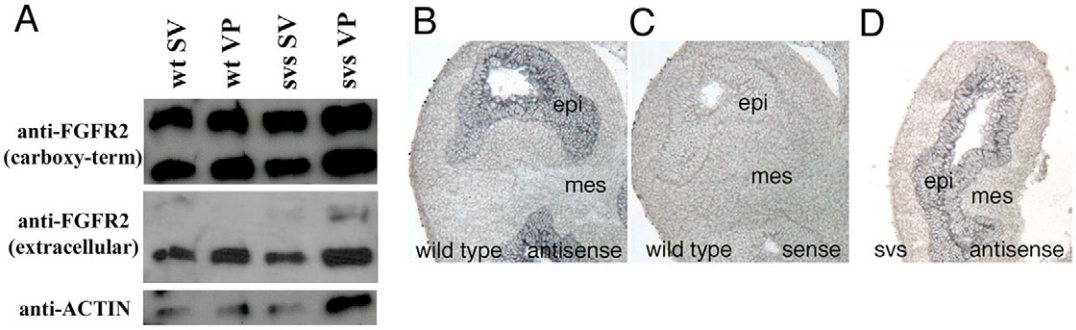

Fig. 3. FGFR2 protein levels and message localization are unchanged in svs mutant mice. (**A**) Western blot of FGFR2 expression using two antibodies that bind to different regions in the protein in ventral prostates (VP) and seminal vesicles (SV) from svs mutant or heterozygous mice. No difference in protein expression is seen. Top, anti-FGFR2 carboxy-terminus; middle, anti-FGFR2 extracellular domain; bottom, actin was used as a loading control. (**B-D**) In situ hybridization using an antisense probe to *Fgfr2* shows positive staining only in the epithelium of P5 seminal vesicles from wild-type (B) or svs mutant (D) mice. No staining was observed using the sense control probe (C). Abbreviations: epi, epithelium; mes, mesenchyme.

UO126, a synthetic inhibitor of MEK1/2 (MAP2K1/2 – Mouse Genome Informatics), the upstream kinases that activate ERK1/2 (Davies et al., 2000). Following 4 days in culture, seminal vesicles cultured with testosterone branched significantly, whereas loss of ERK1/2 activation due to UO126 led to a complete loss of branching morphogenesis (Fig. 6C,D). These effects were unlikely to be due to interference with androgen receptor signaling because the levels of activated ERK1/2 were indistinguishable in organs cultured with or without testosterone (Fig. 6D). These data demonstrated that activation of the MEK1/2-ERK1/2 signaling pathway downstream of FGFR2(IIIb) is crucial for branching morphogenesis in the developing seminal vesicles. These data are also consistent with the possibility that the loss of ERK1/2 activation in svs mutant seminal vesicles is the proximal mechanism responsible for defects in branching morphogenesis.

Previous in vitro studies using recombinant FGF10 to treat prostatic organ cultures have suggested that FGF10 regulates the expression of several genes implicated as regulators of branching morphogenesis in the prostate and/or seminal vesicles (Huang et al., 2005). We used real time RT-PCR to evaluate the effects of partial loss of FGFR2(IIIb) on the expression of branching-regulatory genes (Fig. 7A-G). Although expression of the upstream ligand *Fgf10* was unaffected, mRNA levels for several other branching regulators, including *Shh*, *Gli1*, *Gli2*, *Ptch1*, *Bmp4* and *Bmp7*, were all reduced in svs mutant seminal vesicles.

DISCUSSION

Here we report that the spontaneous recessive mutation in svs mutant mice is a unique hypomorphic allele of *Fgfr2* caused by a 491 bp insertion in intron 10 of the *Fgfr2* gene. The insertion sequence is identical to a murine leukemia virus long terminal repeat (Fig. 2). This mutant lesion is consistent with previous studies which have shown that ~10% of spontaneous mutations in mice are due to transposable elements, including many instances of de novo murine leukemia virus insertion (Maksakova et al., 2006). The main effect of this insertion in the developing seminal vesicles is to change the pattern of alternative splicing of the *Fgfr2* transcript (Figs 3, 4). During seminal vesicle development, the epithelium expresses *Fgfr2* transcripts containing exon 8IIIb, whereas transcripts containing exon 8IIIc are absent. In other tissues, mesenchymal cells express transcripts containing exon 8IIIc. The aberrant alternative splicing in svs mutant mice does not appear to change the primary localization pattern of *Fgfr2* transcripts in the seminal vesicles; in situ hybridization using a probe containing sequences found in all isoforms of *Fgfr2* exhibited epithelial-specific localization in both wild-type and svs mutants (Fig. 3). However, the presence of low levels of *Fgfr2* transcripts containing exon 8IIIc in the mesenchyme cannot be ruled out. In situ hybridization was conducted using probes specific to exon 8IIIb and exon 8IIIc of *Fgfr2*, but these probes were not sensitive enough to detect *Fgfr2* transcripts in svs mutant seminal vesicles (data not shown).

The change in alternative splicing presumably results from the disruption of primary sequence, or from secondary structure elements within the *Fgfr2* pre-mRNA that are required for the highly regulated and complex pattern of *Fgfr2* alternative splicing previously described (Ingersoll et al., 2001). Alternative usage of exon 8IIIb and 8IIIc is regulated by cis elements present in the intronic sequences between exon 8IIIb and 8IIIc that are recognized by transactivating factors such as FOX-2 (RBM9 – Mouse Genome Informatics) (Baraniak et al., 2006). It is possible that the svs mutation disrupts these cis-acting regulatory sequences thereby blocking the recruitment of important transactivating splicing factors. However, the svs insertion is approximately 2 kb 3′ of known *Fgfr2* splicing-regulatory elements, including IAS1 (intronic activating sequence), ISAR (intronic splicing activator and repressor), IAS1 (intronic activating sequences 1), IAS2, IAS3, ISE1 (intronic silencing enhancers 1), ISE2 and ISE3 (Baraniak et al., 2006; Baraniak et al., 2003; Hovhannisyan and Carstens, 2005). Thus, the svs mutation may indicate the presence of one or more previously unrecognized intronic regulatory splicing elements in the tenth intron of *Fgfr2*.

During our analysis of *Fgfr2* transcripts present during branching morphogenesis in wild-type organs, we identified 11 distinct splice variants (Fig. 4B). Although the importance of alternative splicing has not been well characterized for many of the alternatively-included *Fgfr2* exons, the alternative usage of exons 8IIIb and 8IIIc has been extensively studied and shown to function as a key determinant of FGFR2 ligand specificity (Ingersoll et al., 2001). All of the wild-type *Fgfr2* transcripts included exon 8IIIb, which is essential for receptor activation by FGF7 and FGF10, the ligands expressed by the prostate and seminal vesicle mesenchyme. In svs mutant organs, 10 of the 11 wild-type *Fgfr2* splice variants were reduced in abundance or absent. The dramatic changes observed in alternative splicing, along with the recessive nature of the svs

A

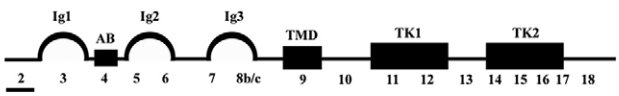

B

		wildtype	svs
1.	2---4-5-6-7-8b-9 -10-11-12-13-14-15-16-17-18s	46(41.5%)	21(21.9%)
2.	2-3-4-5-6-7-8b-9 -10-11-12-13-14-15-16-17-18s	27(25.5%)	0(0%)
3.	2-----5-6-7-8b-9 -10-11-12-13-14-15-16-17-18s	11(10.4%)	22(22.9%)
4.	2---4-5-6-7-8b-9* -10-11-12-13-14-15-16-17-18s	11(10.4%)	6(6.3%)
5.	2---4-5-6-7-8b-9 -10-11-12-13-14-15-16-17-18l	5(4.7%)	0(0%)
6.	2-----5-6-7-8b-9* -10-11-12-13-14-15-16-17-18s	3(2.8%)	0(0%)
7.	2-3-4-5-6-7-8b-9* -10-11-12-13-14-15-16-17-18s	2(1.9%)	0(0%)
8.	2-3-4-5-6-7-8b-9 -10-11-12-13-14-15-16-17-18l	2(1.9%)	0(0%)
9.	2---4-5-6-7-8b-9**-10-11-12-13-14-15-16-17-18s	1(0.9%)	0(0%)
10.	2-----5-6-7-8b-9* -10-11-12-13-14-15-16-17-18l	1(0.9%)	0(0%)
11.	2--4-5-6-7-8b-8c-9-10-11-12-13-14-15-16-17-18s	1(0.9%)	0(0%)
12.	2---------7-8c-9 -10-11-12-13-14-15-16-17-18s	0(0%)	1(1.0%)
13.	2-----5-6-7-8c-9* -10-11-12-13-14-15-16-17-18l	0(0%)	1(1.0%)
14.	2-3-4-5-6-7-8c-9* -10-11-12-13-14-15-16-17-18s	0(0%)	1(1.0%)
15.	2-----5-6-7-8b-9 -10-11-12-13-14-15-16-17-18l	0(0%)	2(2.1%)
16.	2---------7-8b-9 -10-11-12-13-14-15-16-17-18s	0(0%)	3(3.1%)
17.	2-3-4-5-6-7-8c-9* -10-11-12-13-14-15-16-17-18s	0(0%)	7(7.3%)
18.	2-----5-6-7-8c-9* -10-11-12-13-14-15-16-17-18s	0(0%)	7(7.3%)
19.	2-----5-6-7-8c-9 -10-11-12-13-14-15-16-17-18s	0(0%)	25(26.0%)

Fig. 4. Dramatic alterations in alternative splicing of *Fgfr2* in svs mutant mice. (**A**) FGFR2 is represented by a schematic of its protein domains with the corresponding exons numbered below each domain. The bar below the diagram indicates the location of the in situ hybridization probe used in Fig. 3. (**B**) The transcript structure of the 19 different isoforms of *Fgfr2* identified in svs mutant and wild-type seminal vesicles, along with the number of times each transcript was found and the percentage of all isoforms identified in parentheses. The complete sequence of each transcript is available from GenBank with accession numbers EF143322-EF143340. Abbreviations: Ig, Immunoglobulin-like; AB, acid box; TMD, transmembrane domain; TK, tyrosine kinase domain; 8b/c, exon 8IIIb or 8IIIc.

phenotypes, suggested that partial loss of FGFR2(IIIb) function was responsible for these svs mutant phenotypes. This was confirmed by the failure of a known null allele of *Fgfr2* to complement the svs mutation (Fig. 5).

A comparison of svs phenotypes with the existing allelic series of *Fgfr2* mutations makes clear that the svs mutation causes only a partial loss of FGFR2 function that results in mild phenotypes relative to other alleles. The svs mutation is adult-viable, with minimal affect on most organ systems outside of the male reproductive tract (Marker et al., 2003a; Shukri et al., 1988). By contrast, many *Fgfr2* loss-of-function mutant alleles result in lethality due to affects on multiple organ systems. *Fgfr2* is known to be required for early mammalian development because an *Fgfr2*-null mutation caused peri-implantation embryonic lethality shortly after embryonic day (E) 4.5 (Arman et al., 1998). A strong hypomorphic *Fgfr2* allele that deleted the exons encoding the immunoglobin-like domain III extracellular ligand-binding domain caused embryonic lethality around E10.5, a failure of limb bud induction, and placental defects (Xu et al., 1998). *Fgfr2(IIIb)*, an isoform-specific knockout allele of *Fgfr2* that eliminated receptor isoforms incorporating exon 8IIIb, caused perinatal lethality with multiple organ defects including a complete failure of developmental growth and branching in the lung (De Moerlooze et al., 2000). Subsequent studies revealed that elimination of *Fgfr2(IIIb)* also caused growth and branching defects in additional organs including the mammary glands and pancreas (Mailleux et al., 2002; Pulkkinen et al., 2003). Although *Fgfr2* has previously been implicated in branching morphogenesis in several organs outside of the male reproductive tract, branching morphogenesis in the seminal vesicles and prostate seem particularly sensitive to the affects of the svs mutation. For example, we have analyzed whole-mount preparations of svs mammary glands and evaluated the histology of svs lungs (data not shown). These efforts did not reveal dramatic branching morphogenesis defects in svs mutants. However, very subtle affects of the svs mutation on branching in these organs might have been missed.

Initial interest in identifying the gene affected by the svs mutation came from the previously described svs phenotypes, which include a complete failure of branching morphogenesis during seminal vesicle development and dramatically reduced branching morphogenesis in the prostate gland without associated defects in organ growth or differentiation (Marker et al., 2003a). Genes from the fibroblast growth factor family, hepatocyte growth factor family, epidermal growth factor family, transforming growth factor beta superfamily, sonic hedgehog pathway and, more recently, notch signaling have all been implicated as regulators of branching morphogenesis (Davies, 2002; Marker et al., 2003b; Wang et al., 2006). However, it is often unclear what precise role each gene plays in controlling branching morphogenesis. Many of the genes are temporally and spatially regulated during development and are likely to regulate multiple steps during organogenesis. The multiple roles of key regulatory genes make it difficult to establish a precise function for each gene during branching morphogenesis.

It has previously been suggested that, in the prostate and seminal vesicles, signaling by FGF7 and FGF10 through FGFR2(IIIb) is important for epithelial proliferation and duct elongation during branching morphogenesis (Thomson, 2001; Thomson and Cunha, 1999). *Fgf7* and *Fgf10* are expressed by the mesenchyme of both the prostate and seminal vesicles during development, and recombinant FGF7 or FGF10 stimulated both growth and branching of developing prostates and seminal vesicles in vitro, acting at least in part as pro-proliferative signals for the epithelium (Alarid et al., 1994; Sugimura et al., 1996; Thomson and Cunha, 1999). The requirement for FGF10 for prostate and seminal vesicle development was confirmed by experiments showing that *Fgf10*-null embryos develop only minimal prostatic organ rudiments and that the caudal segments of the Wolffian ducts, which are the precursor structures for the seminal vesicles, degenerate in a majority of *Fgf10*-null embryos (Donjacour et al., 2003). Additionally, grafting of embryonic prostates revealed that minimal prostate development occurred from *Fgf10*-null prostates. Similarly, grafting the caudal Wolffian ducts from the rare *Fgf10*-null embryos in which they did not degenerate, revealed that *Fgf10*-null embryos had a limited ability to develop rudimentary seminal vesicles, with only one in eight grafted Wolffian ducts resulting in tissue that resembled immature seminal vesicle (Donjacour et al., 2003).

The fact that prostates and seminal vesicles exhibit no size deficit in svs mutant mice (Marker et al., 2003a), whereas *Fgf10*-null embryos exhibit a dramatic loss of growth for both organs, suggests that FGF10 can partially signal through the reduced levels of FGFR2(IIIb) still present in svs mutant organs and that this is sufficient to support organ growth. However, branching morphogenesis fails completely in svs seminal vesicles and is reduced by ~40% in svs prostates (Marker et al., 2003a). This

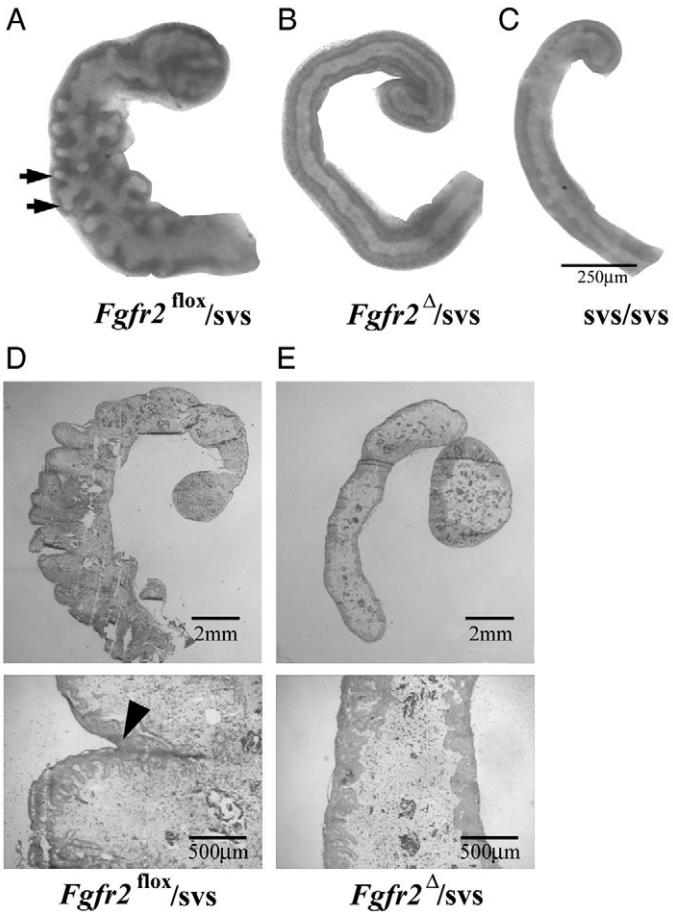

Fig. 5. The svs mutation is allelic with *Fgfr2*. A genetic complementation test to determine if svs is an allele of *Fgfr2*. (**A**) P5 seminal vesicles from *Fgfr2*^{flox}/svs mice initiated normal branching morphogenesis indicating that a functional *Fgfr2* gene complements the svs mutation. Arrows indicate branched tips of the seminal vesicle. (**B**) Conversely, p5 seminal vesicles from *Fgfr2*$^{\Delta}$/svs mice failed to initiate branching morphogenesis, indicating that a null allele of *Fgfr2* fails to complement the svs mutation. (**C**) A p5 svs homozygous mutant seminal vesicle is shown for comparison. (**D**,**E**) Frozen sections of seminal vesicles from fully developed *Fgfr2*^{flox}/svs and *Fgfr2*$^{\Delta}$/svs adult mice were stained with Hematoxylin and Eosin. (D) Upper image depicts a cross-section of seminal vesicles from *Fgfr2*^{flox}/svs mice with a complex branched structure. The bottom image shows the same seminal vesicle at increased magnification showing the presence of macroscopic clefts (arrowhead) that result from developmental branching morphogenesis. (E) Upper image depicts seminal vesicles from *Fgfr2*$^{\Delta}$/svs mice that lack all branching. The bottom image shows the same seminal vesicle at increased magnification showing the lack of macroscopic clefts.

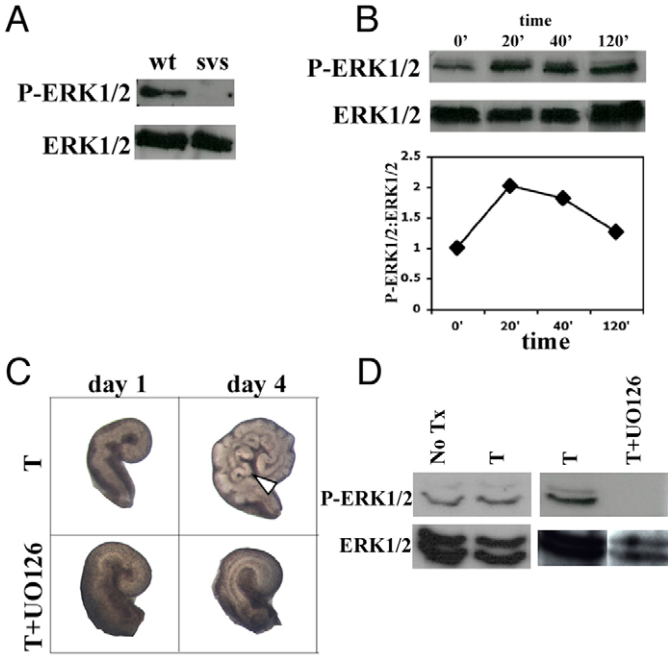

Fig. 6. Signal transduction through the MEK/ERK pathway is defective in svs mutant mice. (**A**) Western blots of P5 seminal vesicles from svs mutant and heterozygous control mice showing the loss of activated ERK1/2 in seminal vesicles from the svs mutant mice. (**B**) Western blot of seminal vesicles from P1 wild-type mice stimulated with recombinant FGF10 protein for 0, 20, 40 or 120 minutes, revealing a 2-fold activation of ERK1/2 by 20 minutes of stimulation, which recedes to near basal levels by 2 hours. Graph below shows quantification of the western blot results. (**C**) P1 wild-type seminal vesicles were cultured in serum-free medium (data not shown), serum-free medium plus testosterone (T), or serum-free medium with testosterone and UO126 (T+UO126). Testosterone stimulates lateral branching during a 4-day culture period (arrowhead). UO126 completely abrogates all testosterone-induced branching (bottom panels). (**D**) Western blot of cultured seminal vesicles confirms that testosterone does not stimulate activation of ERK1/2, and that UO126 inhibits ERK1/2 phosphorylation.

suggests that peak levels of FGF10 signaling through FGFR2 are required to induce branching because partial loss of FGFR2(IIIb) in svs mutant mice blocked branching in the seminal vesicles and reduced branching in the prostate. FGFR2(IIIb) can activate several downstream signaling pathways. This study highlights the importance of the MEK1/2-ERK1/2 signaling pathway in branching morphogenesis. The svs mutant seminal vesicles failed to maintain activation of the MEK1/2-ERK1/2 pathway during branching morphogenesis despite similar overall levels of FGFR2 protein expression in wild-type and mutant seminal vesicles. The loss of ERK1/2 activation is likely to result from the shift in *Fgfr2* alternative splicing that decreases the abundance of exon 8(IIIb)-containing isoforms and results in the ectopic expression of exon 8(IIIc) isoforms that are normally not expressed during seminal vesicle development (Fig. 4). FGF7 and FGF10 are thought to be the ligands that activate FGFR2 during seminal vesicle and prostate development (Thomson, 2001; Thomson and Cunha, 1999). Since these ligands cannot signal via exon 8(IIIc)-containing FGFR2 isoforms, the partial loss of exon 8(IIIb)-containing isoforms may be sufficient to explain the loss of ERK1/2 activation in svs mutant seminal vesicles. Previous studies have also shown that different isoforms of FGFR2 can heterodimerize (Tanahashi et al., 1996), suggesting that heterodimers between exon 8(IIIb)-containing and exon 8(IIIc)-containing FGFR2 isoforms in svs organs may further reduce the availability of functional receptors for FGF7 and FGF10. It is also possible that the ectopic expression of 8(IIIc)-containing FGFR2 isoforms in svs mutant mice could cause gain-of-function phenotypes owing to signaling through other known FGFR2 downstream signaling pathways such as p38 MAPK, AKT or PLCγ (Ceridono et al., 2005; Chen et al., 2000; Mehta et al., 2001).

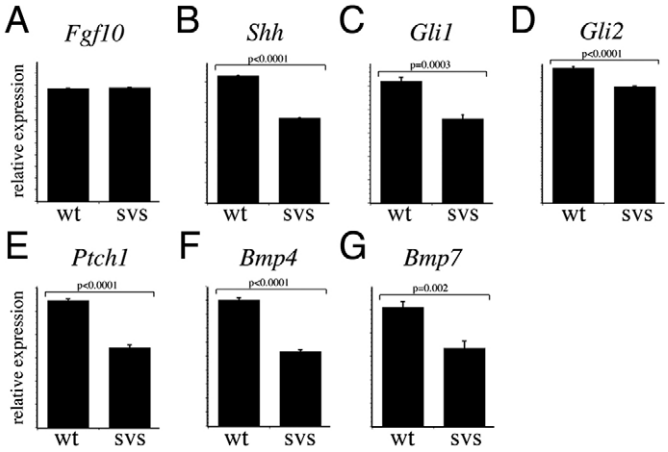

Fig. 7. Gene expression defects in svs mutant mice. (**A-G**) Real time RT-PCR comparison of mRNA levels in littermate control and svs homozygous mutant P5 seminal vesicles for genes implicated as branching morphogenesis regulators in the prostate and/or seminal vesicles. Bar graphs show the ratio of gene expression relative to 18S RNA expression; error bars show s.d. for three replicates of each measurement. Expression of *Fgf10* was the same in wild-type and svs mutant mice (A). Expression of *Shh* (B), *Gli1* (C), *Gli2* (D), *Ptch1* (E), *Bmp4* (F) and *Bmp7* (G) were reduced in svs mutant mice as compared with wild-type animals. Differences observed in B-G were statistically significant (ANOVA test with least significant difference post-hoc analysis; *P* value shown above each graph).

However, the failure of an *Fgfr2*-null mutation to complement svs developmental phenotypes (Fig. 5) confirms that the loss-of-function effects of the svs mutation on FGFR2 are responsible for those phenotypes.

Since svs mutant mice only display defects in the process of branching morphogenesis in the prostate and seminal vesicles, we were able to identify downstream changes that are associated specifically with *Fgfr2*-stimulated branching morphogenesis. We found that decreased FGFR2(IIIb) signaling lead to reduced mRNA expression for six genes previously implicated as regulators of branching morphogenesis in the prostate, and this might be indicative of a more global change in the expression of branching morphogenetic regulators (Fig. 7B-G) (Grishina et al., 2005; Lamm et al., 2001; Podlasek et al., 1999; Pu et al., 2004). These data provide genetic support for previous in vitro studies that have suggested cross-regulation among branching morphogenesis-regulatory genes. Many of the gene expression changes observed in our experiments could be predicted from previous in vitro studies. For example, short-term treatment of ventral and lateral prostates with recombinant FGF10 upregulated expression of *Shh*, *Ptch1*, *Gli1*, *Gli2* and *Bmp7*, and our experiments showed that a partial loss of FGFR2(IIIb), the FGF10 receptor, resulted in decreased expression of these genes (Huang et al., 2005). However, our studies did not always perfectly mirror the results predicted by short-term in vitro experiments. For example, short-term treatment of ventral and lateral prostates with recombinant FGF10 downregulated expression of *Bmp4*, and our experiments showed that a partial loss of FGFR2(IIIb) also resulted in decreased expression of *Bmp4* (Huang et al., 2005). This difference in the effects of FGFR2(IIIb) signaling on *Bmp4* expression between the in vitro organ cultures and the in vivo organs is likely to be due to the different time frames that the organs are exposed to the increased or decreased receptor activity before examining transcript levels. For the in vitro organ cultures, the ventral prostate and lateral prostate were treated with recombinant FGF10 for 24 hours, then RNA was extracted and transcript levels determined (Huang et al., 2005). This time frame is short compared with the situation for the seminal vesicles from the svs mutant mice, which experienced decreased FGFR2(IIIb) signaling throughout organogenesis. Furthermore, it is likely that branching morphogenesis regulators participate in feedback loops that are reiteratively used during ductal elongation and branching, such that long-term loss of a key gene such as *Fgfr2(IIIb)* would cause a general downregulation of the branching process and its associated gene expression.

Conclusions

The mouse svs mutation causes a complete loss of branching morphogenesis in the seminal vesicles and a dramatic reduction of branching in the prostate without changes to organ growth or differentiation. These phenotypes are caused by a 491 bp insertion in the tenth intron of *Fgfr2*, which is associated with aberrant alternative splicing that alters receptor activity without affecting protein expression levels or transcript localization. The partial loss of 8IIIb-containing transcripts is responsible for svs phenotypes because a null allele of *Fgfr2* failed to complement the svs mutation. Furthermore, the reduced FGFR2(IIIb) activity caused a loss of sustained ERK1/2 activation and a reduction in the transcript levels of *Shh*, *Ptch1*, *Gli1*, *Gli2*, *Bmp4* and *Bmp7*, which are important regulators of branching morphogenesis. Thus, the svs mutation provides a unique model to study branching morphogenesis of the prostate and seminal vesicles and FGFR2 function during development and in the adult.

We thank D. Ornitz for providing *Fgfr2* flox mice; Y. Zhang for help with statistical analysis of data; J. Westendorf, L. Collier, D. Largaespada, M. Joesting and E. Rahrmann for critical reading of the manuscript. This work was supported by awards 3353-9225-04 from the Minnesota Medical Foundation (P.C.M.), PC030537 from the Department of Defense Congressionally Directed Medical Research Programs (to P.C.M.), AG024278 from the NIH/NIA (to P.C.M.), and Cancer Biology Training Grant CA09138 from the National Institutes of Health (to S.L.K.).

References

Affolter, M., Bellusci, S., Itoh, N., Shilo, B., Thiery, J. P. and Werb, Z. (2003). Tube or not tube: remodeling epithelial tissues by branching morphogenesis. *Dev. Cell* **4**, 11-18.

Alarid, E. T., Rubin, J. S., Young, P., Chedid, M., Ron, D., Aaronson, S. A. and Cunha, G. R. (1994). Keratinocyte growth factor functions in epithelial induction during seminal vesicle development. *Proc. Natl. Acad. Sci. USA* **91**, 1074-1078.

Arman, E., Haffner-Krausz, R., Chen, Y., Heath, J. K. and Lonai, P. (1998). Targeted disruption of fibroblast growth factor (FGF) receptor 2 suggests a role for FGF signaling in pregastrulation mammalian development. *Proc. Natl. Acad. Sci. USA* **95**, 5082-5087.

Arman, E., Haffner-Krausz, R., Gorivodsky, M. and Lonai, P. (1999). Fgfr2 is required for limb outgrowth and lung-branching morphogenesis. *Proc. Natl. Acad. Sci. USA* **96**, 11895-11899.

Baraniak, A. P., Lasda, E. L., Wagner, E. J. and Garcia-Blanco, M. A. (2003). A stem structure in fibroblast growth factor receptor 2 transcripts mediates cell-type-specific splicing by approximating intronic control elements. *Mol. Cell. Biol.* **23**, 9327-9337.

Baraniak, A. P., Chen, J. R. and Garcia-Blanco, M. A. (2006). Fox-2 mediates epithelial cell-specific fibroblast growth factor receptor 2 exon choice. *Mol. Cell. Biol.* **26**, 1209-1222.

Birney, E., Andrews, D., Caccamo, M., Chen, Y., Clarke, L., Coates, G., Cox, T., Cunningham, F., Curwen, V., Cutts, T. et al. (2006). Ensembl 2006. *Nucleic Acids Res.* **34**, D556-D561.

Ceridono, M., Belleudi, F., Ceccarelli, S. and Torrisi, M. R. (2005). Tyrosine 769 of the keratinocyte growth factor receptor is required for receptor signaling but not endocytosis. *Biochem. Biophys. Res. Commun.* **327**, 523-532.

Chen, Y., Li, X., Eswarakumar, V. P., Seger, R. and Lonai, P. (2000). Fibroblast growth factor (FGF) signaling through PI 3-kinase and Akt/PKB is required for embryoid body differentiation. *Oncogene* **19**, 3750-3756.

Davies, J. A. (2002). Do different branching epithelia use a conserved developmental mechanism? *BioEssays* **24**, 937-948.
Davies, S. P., Reddy, H., Caivano, M. and Cohen, P. (2000). Specificity and mechanism of action of some commonly used protein kinase inhibitors. *Biochem. J.* **351**, 95-105.
De Moerlooze, L., Spencer-Dene, B., Revest, J., Hajihosseini, M., Rosewell, I. and Dickson, C. (2000). An important role for the IIIb isoform of fibroblast growth factor receptor 2 (FGFR2) in mesenchymal-epithelial signalling during mouse organogenesis. *Development* **127**, 483-492.
Donjacour, A. A., Thomson, A. A. and Cunha, G. R. (2003). FGF-10 plays an essential role in the growth of the fetal prostate. *Dev. Biol.* **261**, 39-54.
Gabay, L., Seger, R. and Shilo, B. Z. (1997). MAP kinase in situ activation atlas during Drosophila embryogenesis. *Development* **124**, 3535-3541.
Grishina, I. B., Kim, S. Y., Ferrara, C., Makarenkova, H. P. and Walden, P. D. (2005). BMP7 inhibits branching morphogenesis in the prostate gland and interferes with Notch signaling. *Dev. Biol.* **288**, 334-347.
Hajihosseini, M. K., Wilson, S., De Moerlooze, L. and Dickson, C. (2001). A splicing switch and gain-of-function mutation in FgfR2-IIIc hemizygotes causes Apert/Pfeiffer-syndrome-like phenotypes. *Proc. Natl. Acad. Sci. USA* **98**, 3855-3860.
Hertz, J. M., Juncker, I., Christensen, L., Ostergaard, J. R. and Jensen, P. K. (2001). [The molecular genetic background of hereditary craniosynostoses and chondrodysplasias]. *Ugeskr. Laeg.* **163**, 4862-4867.
Hovhannisyan, R. H. and Carstens, R. P. (2005). A novel intronic cis element, ISE/ISS-3, regulates rat fibroblast growth factor receptor 2 splicing through activation of an upstream exon and repression of a downstream exon containing a noncanonical branch point sequence. *Mol. Cell. Biol.* **25**, 250-263.
Huang, L., Pu, Y., Alam, S., Birch, L. and Prins, G. S. (2005). The role of Fgf10 signaling in branching morphogenesis and gene expression of the rat prostate gland: lobe-specific suppression by neonatal estrogens. *Dev. Biol.* **278**, 396-414.
Ingersoll, R. G., Paznekas, W. A., Tran, A. K., Scott, A. F., Jiang, G. and Jabs, E. W. (2001). Fibroblast growth factor receptor 2 (FGFR2): genomic sequence and variations. *Cytogenet. Cell Genet.* **94**, 121-126.
Kim, H. J., Kim, J. H., Bae, S. C., Choi, J. Y. and Ryoo, H. M. (2003). The protein kinase C pathway plays a central role in the fibroblast growth factor-stimulated expression and transactivation activity of Runx2. *J. Biol. Chem.* **278**, 319-326.
Lamm, M. L., Podlasek, C. A., Barnett, D. H., Lee, J., Clemens, J. Q., Hebner, C. M. and Bushman, W. (2001). Mesenchymal factor bone morphogenetic protein 4 restricts ductal budding and branching morphogenesis in the developing prostate. *Dev. Biol.* **232**, 301-314.
Lee, T., Hacohen, N., Krasnow, M. and Montell, D. J. (1996). Regulated Breathless receptor tyrosine kinase activity required to pattern cell migration and branching in the Drosophila tracheal system. *Genes Dev.* **10**, 2912-2921.
Lewandoski, M., Meyers, E. N. and Martin, G. R. (1997). Analysis of Fgf8 gene function in vertebrate development. *Cold Spring Harb. Symp. Quant. Biol.* **62**, 159-168.
Lu, W., Luo, Y., Kan, M. and McKeehan, W. L. (1999). Fibroblast growth factor-10. A second candidate stromal to epithelial cell andromedin in prostate. *J. Biol. Chem.* **274**, 12827-12834.
Mailleux, A. A., Spencer-Dene, B., Dillon, C., Ndiaye, D., Savona-Baron, C., Itoh, N., Kato, S., Dickson, C., Thiery, J. P. and Bellusci, S. (2002). Role of FGF10/FGFR2b signaling during mammary gland development in the mouse embryo. *Development* **129**, 53-60.
Maksakova, I. A., Romanish, M. T., Gagnier, L., Dunn, C. A., van de Lagemaat, L. N. and Mager, D. L. (2006). Retroviral elements and their hosts: insertional mutagenesis in the mouse germ line. *PLoS Genet.* **2**, e2.
Marker, P. C., Dahiya, R. and Cunha, G. R. (2003a). Spontaneous mutation in mice provides new insight into the genetic mechanisms that pattern the seminal vesicles and prostate gland. *Dev. Dyn.* **226**, 643-653.
Marker, P. C., Donjacour, A. A., Dahiya, R. and Cunha, G. R. (2003b). Hormonal, cellular, and molecular control of prostatic development. *Dev. Biol.* **253**, 165-174.
Mehta, P. B., Robson, C. N., Neal, D. E. and Leung, H. Y. (2001). Keratinocyte growth factor activates p38 MAPK to induce stress fibre formation in human prostate DU145 cells. *Oncogene* **20**, 5359-5365.
Nakamura, T., Mochizuki, Y., Kanetake, H. and Kanda, S. (2001). Signals via FGF receptor 2 regulate migration of endothelial cells. *Biochem. Biophys. Res. Commun.* **289**, 801-806.
Newberry, E. P., Willis, D., Latifi, T., Boudreaux, J. M. and Towler, D. A. (1997). Fibroblast growth factor receptor signaling activates the human interstitial collagenase promoter via the bipartite Ets-AP1 element. *Mol. Endocrinol.* **11**, 1129-1144.
Podlasek, C. A., Barnett, D. H., Clemens, J. Q., Bak, P. M. and Bushman, W. (1999). Prostate development requires Sonic hedgehog expressed by the urogenital sinus epithelium. *Dev. Biol.* **209**, 28-39.
Pu, Y., Huang, L. and Prins, G. S. (2004). Sonic hedgehog-patched Gli signaling in the developing rat prostate gland: lobe-specific suppression by neonatal estrogens reduces ductal growth and branching. *Dev. Biol.* **273**, 257-275.
Pulkkinen, M. A., Spencer-Dene, B., Dickson, C. and Otonkoski, T. (2003). The IIIb isoform of fibroblast growth factor receptor 2 is required for proper growth and branching of pancreatic ductal epithelium but not for differentiation of exocrine or endocrine cells. *Mech. Dev.* **120**, 167-175.
Robertson, S. C., Meyer, A. N., Hart, K. C., Galvin, B. D., Webster, M. K. and Donoghue, D. J. (1998). Activating mutations in the extracellular domain of the fibroblast growth factor receptor 2 function by disruption of the disulfide bond in the third immunoglobulin-like domain. *Proc. Natl. Acad. Sci. USA* **95**, 4567-4572.
Sakaguchi, K., Lorenzi, M. V., Bottaro, D. P. and Miki, T. (1999). The acidic domain and first immunoglobulin-like loop of fibroblast growth factor receptor 2 modulate downstream signaling through glycosaminoglycan modification. *Mol. Cell. Biol.* **19**, 6754-6764.
Schmahl, J., Kim, Y., Colvin, J. S., Ornitz, D. M. and Capel, B. (2004). Fgf9 induces proliferation and nuclear localization of FGFR2 in Sertoli precursors during male sex determination. *Development* **131**, 3627-3636.
Settle, S., Marker, P., Gurley, K., Sinha, A., Thacker, A., Wang, Y., Higgins, K., Cunha, G. and Kingsley, D. M. (2001). The BMP family member Gdf7 is required for seminal vesicle growth, branching morphogenesis, and cytodifferentiation. *Dev. Biol.* **234**, 138-150.
Shukri, N. M., Grew, F. and Shire, J. G. (1988). Recessive mutation in a standard recombinant-inbred line of mice affects seminal vesicle shape. *Genet. Res.* **52**, 27-32.
Sugimura, Y., Foster, B. A., Hom, Y. K., Lipschutz, J. H., Rubin, J. S., Finch, P. W., Aaronson, S. A., Hayashi, N., Kawamura, J. and Cunha, G. R. (1996). Keratinocyte growth factor (KGF) can replace testosterone in the ductal branching morphogenesis of the rat ventral prostate. *Int. J. Dev. Biol.* **40**, 941-951.
Sutherland, D., Samakovlis, C. and Krasnow, M. A. (1996). branchless encodes a Drosophila FGF homolog that controls tracheal cell migration and the pattern of branching. *Cell* **87**, 1091-1101.
Tanahashi, T., Suzuki, M., Imamura, T. and Mitsui, Y. (1996). Identification of a 79-kDa heparin-binding fibroblast growth factor (FGF) receptor in rat hepatocytes and its correlation with the different growth responses to FGF-1 between hepatocyte subpopulations. *J. Biol. Chem.* **271**, 8221-8227.
Thomson, A. A. (2001). Role of androgens and fibroblast growth factors in prostatic development. *Reproduction* **121**, 187-195.
Thomson, A. A. and Cunha, G. R. (1999). Prostatic growth and development are regulated by FGF10. *Development* **126**, 3693-3701.
Thut, C. J., Rountree, R. B., Hwa, M. and Kingsley, D. M. (2001). A large-scale in situ screen provides molecular evidence for the induction of eye anterior segment structures by the developing lens. *Dev. Biol.* **231**, 63-76.
Wang, X. D., Leow, C. C., Zha, J., Tang, Z., Modrusan, Z., Radtke, F., Aguet, M., de Sauvage, F. J. and Gao, W. Q. (2006). Notch signaling is required for normal prostatic epithelial cell proliferation and differentiation. *Dev. Biol.* **290**, 66-80.
Waterston, R. H., Lindblad-Toh, K., Birney, E., Rogers, J., Abril, J. F., Agarwal, P., Agarwala, R., Ainscough, R., Alexandersson, M., An, P. et al. (2002). Initial sequencing and comparative analysis of the mouse genome. *Nature* **420**, 520-562.
Xiao, L., Naganawa, T., Obugunde, E., Gronowicz, G., Ornitz, D. M., Coffin, J. D. and Hurley, M. M. (2004). Stat1 controls post natal bone formation by regulating FGF signaling in osteoblasts. *J. Biol. Chem.* **279**, 27743-27752.
Xu, X., Weinstein, M., Li, C., Naski, M., Cohen, R. I., Ornitz, D. M., Leder, P. and Deng, C. (1998). Fibroblast growth factor receptor 2 (FGFR2)-mediated reciprocal regulation loop between FGF8 and FGF10 is essential for limb induction. *Development* **125**, 753-765.
Yan, G., McBride, G. and McKeehan, W. L. (1993). Exon skipping causes alteration of the COOH-terminus and deletion of the phospholipase C gamma 1 interaction site in the FGF receptor 2 kinase in normal prostate epithelial cells. *Biochem. Biophys. Res. Commun.* **194**, 512-518.
Yan, X., Yokote, H., Jing, X., Yao, L., Sawada, T., Zhang, Y., Liang, S. and Sakaguchi, K. (2005). Fibroblast growth factor 23 reduces expression of type IIa Na+/Pi co-transporter by signaling through a receptor functionally distinct from the known FGFRs in opossum kidney cells. *Genes Cells* **10**, 489-502.
Yu, K., Xu, J., Liu, Z., Sosic, D., Shao, J., Olson, E. N., Towler, D. A. and Ornitz, D. M. (2003). Conditional inactivation of FGF receptor 2 reveals an essential role for FGF signaling in the regulation of osteoblast function and bone growth. *Development* **130**, 3063-3074.